Journal of Physics and Chemistry of Solids 121 (2018) 139–144

Contents lists available at ScienceDirect

Journal of Physics and Chemistry of Solids

journal homepage: www.elsevier.com/locate/jpcs

Structural, elastic, electronic, phonon, dielectric and optical properties of Bi_3TeBO_9 from first-principles calculations

Mi Zhong[a,b], Qi-Jun Liu[a,b,*], Cheng-Lu Jiang[a,b], Fu-Sheng Liu[a,b], Bin Tang[c], Xiao-Juan Peng[d]

[a] School of Physical Science and Technology, Southwest Jiaotong University, Key Laboratory of Advanced Technologies of Materials, Ministry of Education of China, Chengdu, 610031, People's Republic of China
[b] Bond and Band Engineering Group, Sichuan Provincial Key Laboratory (for Universities) of High Pressure Science and Technology, Southwest Jiaotong University, Chengdu, 610031, People's Republic of China
[c] State Key Laboratory of Solidification Processing, Northwestern Polytechnical University, Xi'an, 710072, People's Republic of China
[d] College of Civil Engineering, Chongqing Jiaotong University, Chongqing, 400074, People's Republic of China

ARTICLE INFO

Keywords:
Bi_3TeBO_9
Electronic structure
Optical properties
First-principles calculations

ABSTRACT

The energy band structure, electronic density of states, elastic constants, phonon spectrum, dielectric and optical properties of Bi_3TeBO_9 (BTBO) were studied by means of the first-principles calculations. The obtained structural parameters from PBEsol functional method are in good agreement with the experiment values. From the elastic constants, the bulk modulus (B), shear modulus (G), Young's modulus (E), Poisson's ratio (ν and ν_{ij}), ratio of B/G and C_{12}-C_{44} have been obtained. The BTBO is found to be ductile. The energy band structure and DOS indicate that the nonlinear optical (NLO) properties are dominated by the electron jumping from the top of the valence bands to the bottom of the conduction bands. The phonon and dielectric properties of BTBO were calculated, indicating that the BTBO is dynamically stable and has relatively high dielectric constant. Moreover, the optical properties such as dielectric function $\varepsilon(\omega)$, refractive index $n(\omega)$, extinction coefficient $k(\omega)$, absorption coefficient $\alpha(\omega)$, optical reflectivity$R(\omega)$ and energy-loss function $L(\omega)$ were calculated and analyzed.

1. Introduction

Nonlinear optical (NLO) materials quickly develop and hitherto remain overwhelming interests, which are extensively used in optoelectronics and lasers [1,2]. In order to better use NLO materials, a lot of researches about NLO effects have been carried out and many significant results are obtained [2–15]. Miller [3] found that the crystals with large linear susceptibilities would show large nonlinear effects. Therefore, the NLO ferroelectric crystals with large linear polarization came into people's vision. However, the origin of NLO effects should be further studied. Hence the origin theories related to bond nonlinearities [4]/bond polarizability [5] have been proposed. The core idea is that the observed bulk nonlinear coefficients are linked with the individual bond polarizabilities [5]. The relative investigations of theoretical models and NLO materials have been widely reported [6–15]. The organic [7,13,14], semi-organic [8,10,11], one-dimensional [9,12], bulk size [15] NLO materials have been shown and analyzed. Recently, Xia et al. firstly reported a promising new NLO material Bi_3TeBO_9 (BTBO) with high second harmonic generation response by using the high temperature solution method [16]. The BTBO crystallizing in a polar hexagonal space group of $P6_3$ has three types of nonlinear optical active units, including Bi^{3+} cations, TeO_6 octahedra and BO_3 groups. They lay the foundation for the investigations of this new NLO material. There is no doubt that many physical and chemical properties should be further investigated to better apply BTBO. Hence, we study the structural, elastic, electronic, phonon, dielectric and optical properties of Bi_3TeBO_9 from first-principles calculations.

2. Computational methods

The first-principles calculations in this paper were performed using the plane-wave ultrasoft pseudopotential method/the norm-conserving pseudopotential method based on the density functional theory as implemented in the CASTEP [17]. The local density approximation (LDA) with CAPZ and generalized gradient approximation (GGA) with PW91, PBE, RPBE, WC and PBEsol functionals [18] were used to describe the exchange-correction interactions. In order to solve the underestimated band gap caused by the LDA/GGA calculations, we used the hybrid functionals with B3LYP, PBE0 and HSE06. We used the ultrasoft pseudopotential (LDA/GGA) and norm-conserving pseudopotential

* Corresponding author. Bond and Band Engineering Group, Sichuan Provincial Key Laboratory (for Universities) of High Pressure Science and Technology, Southwest Jiaotong University, Chengdu, 610031, People's Republic of China.
E-mail address: qijunliu@home.swjtu.edu.cn (Q.-J. Liu).

https://doi.org/10.1016/j.jpcs.2018.05.026
Received 27 February 2018; Received in revised form 11 May 2018; Accepted 17 May 2018
Available online 18 May 2018
0022-3697/

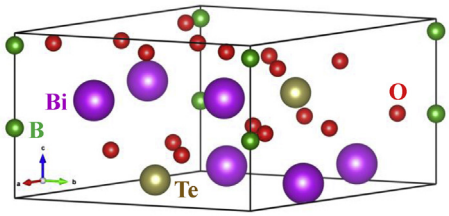

Fig. 1. Crystal structure of BTBO.

(B3LYP/PBE0/HSE06) to treat the electron-ion interactions. According to the previous research [19], the HSE06 functional was the best choice for the calculation of electronic properties due to the reasonable choice of the coulomb screen parameter. In order to obtain the better electronic properties, the good amount of nonlocal exchange should be given by the coulomb screen parameter. The Te $5s^2 5p^4$, B $2s^2 2p^1$, Bi $6s^2 6p^3$ and O $2s^2 2p^4$ electrons were treated as valence states. The Brillouin zone (BZ) for the calculations was sampled with the Monkhorst Pack mesh ($2 \times 2 \times 2$) [20]. The convergence criterion of the change in total energy was less than 5.0×10^{-6} eV/atom. Moreover, the density functional perturbation theory (DFPT) was used to calculate the phonon and dielectric properties.

3. Results and discussion

3.1. Structural parameters

The BTBO with hexagonal space group $P6_3$ is shown in Fig. 1. The Bi^{3+} cations occupy (0.29827(3),0.34622(3),0.10689(12)) site, which are bonded to six O atoms to form the distorted BiO_6 octahedra [16]. The Te^{6+} cations are located at (2/3,1/3,0.0813 (2)) site, which also bonded to six O atoms to constitute the TeO_6 octahedra [16]. The B atoms are at (0,0,0.425 (3)) site and three different types of O atoms are at O1 (0.4599(9),0.2464(9),0.2679(12)), O2 (0.5407(8),0.4147(8),-0.1042(13)) and O3 (0.1009(9),0.1813(8),0.4333(13)) [16]. The calculated structural parameters along with the experimental data [16] of BTBO are shown in Table 1. Compared with the experimental values, the obtained structural parameters with LDA calculations are obviously underestimated, and the results based on GGA calculations with PBE, RPBE and PW91 functionals are overestimated. The calculated values based on WC and PBEsol functionals are in good agreement with experimental data. In the following works, we choose the GGA-PBEsol functional to calculate physical properties.

3.2. Elastic and mechanical properties

It is well known that the response of a solid under external forces is associated with the elastic constants which can be used to judge the mechanical stability. In order to explore the mechanical properties of BTBO, the elastic constants are calculated and shown in Table 2. The hexagonal BTBO has five independent elastic constants, including C_{11}, C_{12}, C_{13}, C_{33} and C_{44}. According to the mechanical stability criteria [21]: $C_{11} > 0$, $C_{33} > 0$, $C_{44} > 0$, $C_{11} > |C_{12}|$, $[(C_{11} + C_{12})C_{33} - 2C_{13}^2] > 0$, we can conclude that the BTBO is mechanically stable.

Table 1
Calculated structural parameters of BTBO along with the experimental values [16].

Phase	*a*	*c*	*V*	
$P6_3$	8.6474	5.6030	362.848	LDA + CA-PZ
	8.9923	5.7962	405.898	GGA + PBE
	9.0740	5.8629	418.059	GGA + RPBE
	8.9950	5.7944	406.006	GGA + PW91
	8.8948	5.7314	392.700	GGA + WC
	8.8951	5.7326	392.811	GGA + PBEsol
	8.7510 (12)	5.8981 (12)	391.163	Expt [16].

Table 2
Calculated elastic constants of BTBO.

C_{11}	C_{12}	C_{13}	C_{33}	C_{44}
128.42	45.34	57.25	117.59	40.68

To investigate the mechanical properties of BTBO, the calculated bulk modulus, shear modulus, Young's modulus, Poisson's ratio, ratio of G/B, and C_{12}-C_{44} are shown in Table 3 using the Voigt-Reuss-Hill (VRH) approximation [22–24]. The bulk modulus, shear modulus, and Young's modulus are found to be 77.122, 38.577 and 99.192 GPa, respectively. The difference between C_{12} and C_{44} (C_{12}-C_{44}), namely Cauchy's pressure, can be used to indicate the brittle/ductile nature of the material [25]. If C_{12}-$C_{44} > 0$, the material is ductile, otherwise it is brittle. The value of Cauchy's pressure is 4.66 GPa, indicating that the BTBO shows ductile nature. The brittle/ductile nature of the material can be also judged by the ratio of G/B. The value of 0.57 is boundary condition for ductile nature and brittle nature of the material. If G/B < 0.57, the material is ductile, otherwise it is brittle [26]. For the BTBO, the value of G/B is 0.500, showing that this material is ductile. The values of −1 and 0.5 of Poisson's ratio represent the material don't change its shape and volume [27], respectively, which are lower and upper bounds of Poisson's ratio. The value of Poisson's ratio is 0.286, meaning that the stability of the volume is stronger than that of the shape. It is corresponding to B > G.

3.3. Band structure and density of states

The band structure of BTBO is shown in Fig. 2. The GGA-PBEsol, B3LYP, PBE0 and HSE06 calculations indicate that the BTBO has an indirect bandgap. The corresponding values are 1.851, 4.588, 4.970 and 4.218 eV. Compared with the experimental value of 3.23 eV [16], it can be seen that the GGA and B3LYP/PBE0/HSE06 results underestimate and overestimate the bandgap. Although the bandgap based on the HSE06 functional is closest to the experimental value, the deviation of 0.988 eV is obvious due to that the spin-orbit coupling is not taken into account for Bi-based materials [28].

The total and partial densities of states based on the HSE06 functional are shown in Fig. 3. The occupied locations of the partial densities of states for O1, O2 and O3 atoms are similar to each other, but the differences between the values of the peaks can be seen from Fig. 3. Of all the peaks near the Fermi level, we can see that the O1-2p states show the highest peak. As presented in Fig. 3, the lowest region is dominated by the Bi-5d, O (1,2,3)-2s, B-2p, Te-5p states with contributions of B-2s and Te-5s states. The middle region is mainly due to the Te-5s and Bi-6s states. From −7.66 eV to Fermi level, there are main three regions. The first region at about −6.44 eV is due to the hybridizations between O-2p and Te-5p, O-2p and B-2p, O-2p and Bi-6p states. The second region from −5.05 to −0.97 eV are mainly governed by the O-2p, Bi-6p states with minor contributions from B-2p and Te-5p. The third region around the peak at −0.31 eV is due to O-2p, Bi-6s and Bi-6p states. The conduction bands near the Fermi level are consisted of p states of Te, B and Bi. The PDOS give important information for the interactions among the states. The orbital hybridizations are obvious among these states. Based on the nonlinear optical theory, the nonlinear optical effect is mainly governed by the top of the valence bands and the bottom of the conduction bands [29]. Lin et al. said that the electrons jump from the top of the valence bands to the bottom of the conduction bands led to the SHG effect [30]. Therefore, the nonlinear optical properties are mainly from the p states of Te, B, Bi and O due to their major contributions to the DOS.